Published in final edited form as:
Alzheimers Dement. 2010 July ; 6(4): 326–333. doi:10.1016/j.jalz.2009.09.005.

Fluorodeoxyglucose positron emission tomography of mild cognitive impairment with clinical follow-up at three years

José V. Pardo, M.D., Ph.D.[a,d], **Joel T. Lee, M.S.E.E.**[a], **Michael A. Kuskowski, Ph.D.**[a,b,d], **Kristin R. Munch, Ph.D.**[f], **John V. Carlis, Ph.D.**[f], **Sohail A. Sheikh, M.D.**[d], **Christa Surerus, M.A.**[a], **Scott M. Lewis, M.D., Ph.D.**[c,e], **J. Riley McCarten, M.D.**[b,e], **Howard Fink, M.D.**[b], **Susan McPherson, Ph.D.**[b,e], **Hemant H. Shah, M.D.**[d], **Susan Rottunda, M.A.**[b], and **Maurice W. Dysken, M.D.**[b,d]

[a] Cognitive Neuroimaging Unit, Minneapolis Veterans Affairs Medical Center

[b] GRECC, Minneapolis Veterans Affairs Medical Center

[c] Brain Sciences Center, Minneapolis Veterans Affairs Medical Center

[d] Department of Psychiatry, University of Minnesota, Minneapolis

[e] Department of Neurology, University of Minnesota, Minneapolis

[f] Department of Computer Science, University of Minnesota, Minneapolis

Abstract

Background—Alzheimer's disease (AD) is the most common dementing illness. Development of effective treatments directed at AD requires an early diagnosis. Mild cognitive impairment (MCI) often heralds AD. Thus, characterizing MCI is fundamental to the early diagnosis of AD.

Participants—Nineteen MCI patients referred from a memory loss clinic and 27 healthy subjects, all followed for 3 years.

Method—Metabolism scans (MCI minus controls) were compared voxel-wise after anatomical normalization and were examined both visually and with a computerized classifier.

Results—Agreement between raters as to whether the individual scans were normal or abnormal was high. Agreement between raters of the eventual clinical diagnosis and baseline metabolic pattern was poor. A computerized classifier was unsuccessful at classifying MCI from normal; however, its performance improved when using only prototypic AD-like MCI scans, indicating the classifier worked well when shared patterns existed in the data. Outcomes on follow-up were 9/19 AD; 5/19 remained MCI; and 5/19 developed dementias other than AD. Both cases of early Lewy body dementia (LBD) showed an AD-like metabolic pattern.

Conclusions—Visual inspection proved reliable in determining normal from abnormal scans; but it proved unreliable at predicting diagnosis on follow-up. Computerized classification of MCI using an AD-like metabolic template (such as derived from the averaged MCI images) showed

Corresponding author: José V. Pardo, M.D., Ph.D.; VAMC; One Veterans Drive; Minneapolis, MN, 55417, USA. 612-467-3164 (phone); 612-725-2249 (FAX); jvpardo@umn.edu.

The authors declare no conflicts of interest.

potential to identify patients that will develop AD. However, the metabolic pattern in early LBD did not differ from that in AD.

Keywords

MCI; PET; support vector machine; brain metabolism; diagnosis; Alzheimer; frontotemporal dementia; Lewy body; aging; classification

1. Introduction

Mild cognitive impairment (MCI) is considered a transitional phase between healthy cognitive aging and Alzheimer's disease (AD). It is diagnosed when a patient (1) has memory complaints; 2) shows a decline greater than 1.5 standard deviations from the age- and education-adjusted mean in declarative memory scores as assessed by neuropsychological testing; 3) has intact general cognition; 4) shows normal activities of daily living; and 5) does not have dementia [1]. From the initial emphasis on verbal memory, now termed amnestic MCI, the concept has been extended to include multiple-domain MCI and single-domain, non-amnestic MCI [2]. Approximately 20% of individuals over age 70 years have MCI with the incidence rising to almost half of those 80 years or older.

Pharmaceutical agents to prevent or treat AD are under development. Such drugs have the greatest opportunity to treat AD before the disease has progressed to the stage where extensive brain damage has occurred. The diagnosis of MCI is a frequent inclusion criterion for such drug studies. It is assumed to represent a prodrome to AD. Therefore, structural and functional characterization of MCI is important to the early diagnosis of AD.

MCI can be distinguished both structurally and functionally from healthy aging. For example, MCI patients show loss of grey matter and enlarged ventricles [3]. The greatest change occurs in the hippocampus and medial temporal cortex, but it can also include medial prefrontal cortex, posterior cingulate cortex (PCC), orbitofrontal cortices, insula; uncus, ([4] and others). Functionally, hypometabolism localizes to the PCC and parietal cortex as well as to the medial temporal lobe [5–13]. In contrast, grey matter density declines during normal aging in the dorsal prefrontal and parietal cortices, [14]. The major decline in brain metabolism with age in healthy subjects localizes to the anterior cingulate cortex (ACC) and adjacent regions ([15] and reviewed therein).

While the changes in MCI differ clearly from healthy aging, MCI patients share many features with AD. At the most basic level, the neuropathology of MCI appears to be that of AD (16–17). Additionally, FDG PET studies have shown that those MCI patients who later develop probable AD show metabolic reductions similar to those found in AD. For example, eight MCI patients who later converted to probable AD showed reduction in the PCC and cinguloparietal cortices at their baseline evaluation [8]. Impaired baseline metabolism in the left parietotemporal region of MCI patients predicted those who progressed over 3 years [18]. During the examination of 30 MCI patients over 16 months, 13 patients showed an AD pattern of hypometabolism, 11 of these converted to AD, while 16 of the 17patients without the AD pattern remained stable [13]. Likewise, in a large series of 284 patients undergoing evaluation for dementia, the pattern of hypometabolism had predictive power. FDG PET was able to predict deterioration over a 3.2 year follow-up period with a sensitivity of 91% and a specificity of 75% [19]. These studies suggest that MCI patients with AD-like metabolic changes tend to progress and convert to AD.

The clinical course of MCI is variable. Overall, MCI patients have greater cognitive decline than normal subjects and show less decline than AD patients [1]. Whereas 1–2% of normal elderly convert to AD per year, approximately 10–15% of MCI patients convert to AD per year. Therefore, MCI represents at least a group at high risk of converting to AD. It is important to note that the original criteria for MCI are based upon a clinical sample, i.e., those presenting to clinicians with memory complaints. These criteria do not perform as well in population based studies where interviewers ask subjects about memory complaints [20–21]. The diagnosis appears unstable in such studies with as many as 25% of MCI subjects reverting to normal during a follow-up interval of 10 years [22].

Imaging studies suggest metabolic heterogeneity within MCI itself. Using FDG PET, only 43% of MCI patients exhibited a pattern consistent with AD [13]. A large multicenter study using 114 MCI patients and 110 healthy elderly subjects found an AD pattern by FDG PET in 79% of multiple-domain MCI patients but only 31% of amnestic MCI patients [7]. Amyloid deposition and hypometabolism as assessed by PET showed concordance in 54% of MCI cases [23]. Similarly, only half of MCI patients showed detectable amyloid deposition or microglial activation as assessed with PET [24].

The present study compared FDG PET images in MCI patients referred from a memory loss clinic with a control, normative database of carefully screened subjects. The objective was to determine whether MCI patients could be reliably classified from healthy controls, and if so, could the follow-up diagnoses be determined by the baseline findings. The MCI and control images were interpreted both visually and also processed though a support vector machine (SVM). SVM uses a kernel function to map the data into an infinite-dimensional space, where a hyperplane can be used to do the separation. This allows SVM models to perform separations even when the boundary between the classes is very complex, and even when classes with few samples or samples have high-dimensionality feature vectors. The patients were followed for 3 years after the PET scan.

2. Methods

2.1. Human subjects

The characterization of the control subjects has been described previously [15]. Briefly, they were recruited from the community and underwent extensive medical and laboratory examination. They were assessed free of lifetime history of psychiatric disorders using a structured diagnostic interview. All magnetic resonance images (MRI) were considered normal for age.

The MCI patients were referred for imaging from the memory loss in the Geriatric, Research, Education, and Clinical Center (GRECC) at the Minneapolis Veterans Affairs Medical Center (MVAMC) in Minneapolis, MN. The diagnosis of MCI was made according to the criteria of Petersen et al. [1] after an extensive evaluation including neuropsychological testing and medical evaluation. All but one female were white male veterans. The ages ranged from 54–85 years (mean = 80).

All subjects gave informed consent approved by the Institutional Review Board (IRB) of both the VAMC and the University of Minnesota. The MVAMC's Radiation Drug Committee (RDRC) also evaluated the protocols and dosimetry for consistency with FDA guidelines.

Because of the possibility that control subjects were incorrectly classified as normal controls and could later become symptomatic for AD [25], all controls were reevaluated at ~2–3 years after the scan using the Minnesota Cognitive Acuity Screen (MCAS, [26]). All of

those screened as cognitively impaired at 2–3 years were removed from the control dataset. The final normal control dataset consisted of 27 subjects (12 females) with ages 41–94 years (mean = 72).

2.2. PET imaging

The methods have been described previously [15]. Briefly, after an overnight fast, subjects received an intravenous injection of ^{18}F-FDG at a dose of 5 mCi/70 kg, as they reclined with eyes closed and ears open in a quiet dark room. After a 30 min uptake period, they were transferred to an ECAT 953B or ECAT Exact scanner (Siemens, Knoxville, TN). Attenuation was measured. No arterial catheters were used for absolute quantitation.

2.3. PET scan processing and analysis

PET scans were adjusted to a whole-brain mean activity and stereotactically normalized using Neurostat (S. Minoshima, University of Washington, Seattle, WA). This software has been validated [27–29] and has been used in several studies of aging and AD [e.g., 7–8,13,15]. Each patient's scan was compared voxel-wise to the normative dataset after age regression to generate difference images. Each control subject's scan was compared to the remainder of the control scans using the leave-one-out method with replacement. The color scale for viewing the data ranged from purple (minimum hypometabolism displayed, $t = -2$) to white (maximal hypometabolism displayed, $t = -6$). One blinded reader (JVP) examined the scans using only the transverse sections. The other blinded reader (MAK) used iiV [30] to examine the images. This program displayed all perspectives (coronal, sagittal, and transverse) containing a point of interest selected by the user.

The patterns of metabolic change were identified visually by the readers according to criteria reported widely [5–13]. The AD pattern was identified by hypometabolism in the medial parietal cortex and lateral parietal regions. The medial parietal involvement could include posterior cingulate, retrosplenial cortex, or precuneus. The lateral parietal regions included mostly inferior parietal regions (supramarginal gyrus) with extension into superior parietal cortex and lateral temporal cortex. The FTD pattern was identified by hypometabolism in anterior/superior temporal cortex and mesial/lateral prefrontal cortex, especially with greater involvement in the left than in the right sides. Because there is no pathognomonic feature for early LBD, no attempt was made to classify it unless occipital hypometabolism was present which occurred in no one.

2.4. Support vector machine

These analyses were done on the first 13 MCI cases and 15 controls. The SVM classifier was run on SVMLight [31] using a radial basis function. The parameters for the function were chosen through cross-validation using a toolkit called LIBSVM [32]. Feature selection was accomplished using the fselect tool which measures the "f-score," a simple calculation used to measure the discrimination between two sets of numbers [33]. The entire brain was re-sampled into 3 ×3 × 3 cubic voxels (voxel dimension = 2.25 mm) to minimize computation time. Two features, lobe and cluster, were defined. The lobar features came from the Talairach daemon yielding 12 regions, six in each hemisphere [34]. A brain lobe was labeled as MCI or normal if ≥50% of the cubes had the label MCI or normal, respectively. The cluster feature used a template based upon the average image of the MCI subjects (Fig. 1). Each cluster or connected region was identified using a t threshold of 2. Each sample cube gave 7 first-order statistics on the counts observed: sum, maximum, minimum, mean, median, standard deviation, and variance. Additional second order features included entropy, energy, contrast, and homogeneity [35]. Classification used a cluster-by-cluster approach as well as a whole-brain approach and leave-one-out cross-validation.

3. Results

3.1. Baseline and follow-up diagnoses of MCI patients at 3 years

Table 1 shows the baseline clinical diagnoses of all MCI patients as well as their diagnoses at 3 years. As noted, 11/19 subjects had amnestic MCI with four of these having deficits in multiple domains. On follow-up at three years, nine of nineteen (47%) MCI patients converted to probable or possible AD. Two of nineteen (~10%) patients converted to probable Lewy body dementia (LDB), one of which was autopsy verified. Another two cases converted to probable FTD. Case p0083 converted to dementia, not otherwise specified. Five of nineteen (26%) remained labeled as MCI. Over the three years, four deaths occurred involving one probable AD case, one definite LBD case (autopsy verified), 1 FTD case, and p0083 (dementia, NOS).

3.2. Visual inspection of the difference images

The two independent blinded raters experienced in PET assessed each difference image as normal or abnormal, and if abnormal, whether having an AD or FTD pattern. This would be the most straight forward approach in a clinical setting. Figure 1 shows the average of all MCI patients minus the average of all normal subjects. This average corresponds to the typical AD-like pattern in the literature. However, heterogeneity in metabolic patterns was evident in individual cases. For an example, Figure 2 shows baseline examinations of three MCI subjects-- one showing the AD-like pattern, one without any pattern, and another with an FTD-like pattern. Table 2 shows the agreement between different rater's classifications. The agreement (kappa, κ) between the initial diagnostic label and the observed PET pattern was low for both raters [JVP: $\kappa = 0.40$, SE = 0.14, $p < 0.006$ (vs. $\kappa = 0$); MAK: $\kappa = 0.55$, SE = 0.13, $p < 0.001$ (vs. $\kappa = 0$)]. The inter-rater agreement for classifying images as normal or not normal was high despite each rater using slightly different approaches to examine the data [(JVP vs. MAK for the rating of all normal subjects as "normal" vs. "not normal: $\kappa = 0.86$, SE = 0.08, $p < 0.001$; i.e., agreement on 43 of 46 normal subjects); (JVP vs. MAK for the rating of all MCI subjects as "normal" vs. "not normal": $\kappa = 0.66$, SE = 0.17, $p < 0.002$; i.e., agreement on 16 of 19 MCI patients)].

To address the issue of whether baseline classification predicted outcome at three years, Table 1 shows the baseline classification by both raters along with the clinical diagnosis at 3 years of follow-up. Seven of nineteen cases (p0047, p0078, p0093, p0094, p0100, p0102, p0106) showed agreement across both raters. Of these, 3 cases (p0094, p0102, and p0106) were classified as normal but were diagnosed on follow-up as probable or possible AD. Cases p0078 and p0093 were classified by both raters as AD, but on follow-up were diagnosed as definite LBD and probable LBD, respectively. Case p0100 was classified by both raters as FTD, and the follow-up diagnosis was FTD. Therefore, baseline classification of MCI scans by visual analysis did not reliably predict outcome at 3 years, particularly in trying to differentiate early AD from early LBD.

3.3 Support vector machine

The clusters were defined based on the average t-image between all MCI (N = 19) subjects contrasted with normal controls (N = 27) to provide an MCI template. Figure 1 shows the individual clusters from this averaged difference image. The first classification experiment used the clinical diagnosis (MCI, normal) to label each scan. Using a $3 \times 3 \times 3$ cubes, whole brain and lobar analysis yielded overall a sensitivity of 62% and a specificity of 83%. Analysis using individual clusters did not work well; each brain was classified as normal.

The second classification approach used training labels based upon the pattern in the image, not on clinical diagnosis. Since MCI criteria may result in a heterogeneous group of patients,

the next classification used prototypic examples. All difference images of each MCI patient vs. controls were reviewed visually. The control images were selected based on their having no significant differences (i.e., $t < 2$) from the rest of the controls (N = 15/27). The MCI images were selected as AD-like based on their having hypometabolism in the PCC and in at least one unilateral parietal lobe (e.g., Fig. 1; N = 5/19; pL0024, pL0025, pL0078, pL0083, and pL0093). The average image of the preselected MCI scans minus pre-selected controls showed only one right parietal focus large enough to use as a cluster (Figure 1, cluster #3, 176 valid cubes). This cluster showed an overall classification accuracy of 90% with 100% sensitivity and 86% specificity. Whole-brain classification with lobar segmentation yielded accuracies between 85–90%. Because of the small number of MCI prototypic scans, a low sensitivity was observed when 2/5 cases were misclassified. These results may be improved with more cases for training.

4. Discussion

4.1. Clinical outcomes at 3 years

As expected, the most frequent outcome was AD (47%) or MCI (26%). Probably with continued follow-up, more of the MCI cases would have converted to AD. Given the age range of the sample, the frequencies of conversion to FTD (~10%) and LBD (~10%) are not inconsistent with other prevalence estimates [36].

4.2. Visual classification of MCI vs. Normal FDG PET scans

There was good inter-rater agreement of FDG PET scans classified by visual inspection as “normal” vs. “not normal.” Assuming most neuropsychiatric disorders have signal-to-noise ratios in the image similar in magnitude to that seen in MCI patients, a clinician could be informed as to whether any specific patient has or does not have a normal scan. This may be helpful when there are no clues to diagnosis or evidence for pathology without other findings. Patients with negative scans are unlikely to progress (discussed in Introduction). However, in the present series, both raters identified 3/19 MCI patients as showing the healthy control pattern, yet at three years, these patients progressed to probable or possible AD.

There was poor agreement for both raters between diagnosis at three years and baseline FDG scans identified by the initial label (MCI vs. Normal) and classified as to PET pattern (Normal, AD, FTD). This suggests that labeling scans as MCI or Normal did not produce a population with consistent patterns in the FDG PET images. Indeed, 26% of the MCI sample on follow-up at three years had probable dementias other than AD. When others have used the AD pattern as a template, a considerable fraction of MCI patients do not show the AD pattern.

The large number of MCI patients who did not convert to AD or did not show the AD hypometabolic pattern appears counter-intuitive given the predominant finding that the pathology of MCI is that of AD [16,17]. The follow-up interval in this study was short, and more cases of conversion to AD would be expected with time. We used diagnoses as endpoints, where longitudinal cognitive scores could show progressive deterioration despite persistence of the MCI diagnosis. Also, clinicians may have referred cases with more complex or atypical presentation; this series was not serial. However, this sample was also different than those studied for pathology. The study by Morris et al. (2001) used CDR 0.5 rather than MCI criteria [16]. The equivalence of these two diagnostic approaches is unclear. In the study by Markesbery (2006), control subjects with Braak stages III or higher were excluded, which could bias the differences between AD and controls [17]. Also, the mean time between diagnosis and death for MCI cases was 2 years. Only four of the cases

presented here died in the subsequent three years. Therefore, MCI is clearly enriched in those who will convert to AD, but patients fitting these criteria can develop other dementias. Differences between MCI groups probably reflect differences in the recruitment method and definitions.

4.3. Support vector machine classification

SVM classification based upon the clinical diagnosis of MCI does not produce a population with a consistent pattern in FDG PET scans. The highest accuracy achieved by cluster classification was 67%, and the highest whole-brain classification was 76%. No model produced both a high sensitivity and a high specificity.

This conclusion is consistent with other published literature. For example, Drezega et al. found only 43% of MCI patients had PET scans suggestive of AD pathology [13]. The study also showed that 85% of those with the hypometabolic AD pattern converted to AD with a mean follow-up of 16 months, while those without such a pattern remained largely stable at follow-up (94%). Similarly, a more recent, large, multi-center study found 76% of multi-domain MCI showed the AD pattern, while only 31% of amnestic MCI showed the pattern [7]. The greater prevalence of the AD pattern in the multiple-domain MCI group is consistent with its more aggressive course compared to purely amnestic MCI [37].

Using structural atrophy as quantitated by grey matter density from structural MRI images from the ADNI dataset, Fan et al. used three groups: AD, MCI, and normal subjects [4]. They trained an SVM classifier to optimally separate AD from normal subjects. Using this classifier, they found that 1/3 of MCI patients did not have the AD pattern of atrophy. The AD-like MCI patients showed greater change scores in the Mini-Mental Status Examination than did the MCI patients without the AD structural pattern. No follow-up was reported. Their approach differed from that here in that the present study did not use AD patients to generate a template but attempted to initially classify MCI from normal controls directly. The improved classification based upon separation of AD from controls (that of Fan et al.) when compared to separation of MCI from controls (the case here) suggests the AD pattern is the dominant feature in MCI. In other words, there is no other metabolic signature in MCI patients.

Indeed, the selection of prototypes from the present dataset helped SVM to classify MCI from normal controls. When MCI images were pre-selected showing at least some prototypic AD-like patterns as well as control images that were clearly void of any signals when compared to the other controls, the best performing models had accuracies of 90% with either lobar or cluster feature analysis even with the limited number of scans after selection. This confirmed that SVM was in fact working properly. The right parietal cluster was the sole feature in the cluster analysis. However, the very small number of images produced by the pre-selection of prototypes yielded poor sensitivities and specificities. The loss of so many images suspicious for artifacts or other signals in selecting prototypic images underscores the importance of preventing motion during scanning, which can be particularly difficult for the elderly (especially since many current scanners do not have LIST mode capabilities, i.e., collection of data in sequential blocks of time enabling recovery of data when motion occurs). Additionally, accurate anatomical standardization becomes more important in the face of increased ventricular and sulcal volumes.

4.4. Limitations of the study

The sample size of 19 MCI patients and 27 control subjects may limit the generalizability of the results. Larger samples would improve computerized classification based on machine learning from exemplars. The MCI subjects were recruited from a memory loss clinic in the

GRECC program at a VA Medical Center. All MCI subjects but one were male. Both the source of the subjects and their gender may limit generalizability of the results to other types of clinics or female subjects. Intersubject registration methods and machine learning algorithms are rapidly evolving and may provide improved signal-to-noise ratios in the processed images. Selection of other SVM parameters and software might improve the robustness of the classification. However, the present implementation worked fine with the selected a priori prototypic images. The results of this study depend also on the technology used for imaging. More modern PET scanners with higher resolution may decrease partial volume effects that directly affect the metabolic data and would likely improve the detectability of medial temporal changes. Finally, elderly patients often take many medications and have comorbid illnesses, both of which could affect the brain metabolic data.

4.5 Conclusions

FDG PET scans from subjects who were normal or diagnosed with MCI could be classified visually as “Normal” or “Not Normal” with good inter-rater agreement. However, classification of the scans from the MCI group into normal, AD, or FTD was less reliable. SVM was unsuccessful at classifying MCI patients from normal subjects. Most likely, the heterogeneity seen at follow-up could account for this. In this sample of MCI patients, 25% developed dementias other than AD during a 3 year follow-up. Therefore, no metabolic signature arose in MCI other than the AD-like pattern. SVM was most successful when using only prototypic normal images or AD-like images from MCI patients indicating that SVM could succeed when there were consistent patterns. The right parietal cortex provided the best classification between MCI scans with AD-like pattern from normal controls. With either whole brain or cluster analysis, the accuracy was about 90%. The designation of MCI enriches a sample that will develop AD, but a significant number of cases will also develop other dementias. Identifying baseline scans as AD or FTD met with only partial success when compared to the follow-up diagnoses at three years. These results suggest that drug trials targeted at AD pathology should pre-select enrollees with AD-like patterns. Nevertheless, patients with LBD showed typical AD patterns which would contaminate the sample unless they were also responsive to the treatment under investigation.

Acknowledgments

This work was supported by NIA RO1 AG120852 and the Alzheimer’s Association. We thank Dr. Satoshi Minoshima (University of Washington, Seattle, WA) for enabling the use of Neurostat.

References

1. Petersen RC, Smith GE, Waring SC, Ivnik RJ, Tangalos EG, Kokmen E. Mild cognitive impairment: Clinical characterization and outcome. Arch Neurol 1999;56:303–08. [PubMed: 10190820]
2. Petersen RC, Doody R, Kurz A, Mohs RC, Morris JC, Rabins PV, et al. Current concepts in mild cognitive impairment. Arch Neurol 2001;58:1985–92. [PubMed: 11735772]
3. Jack CR Jr, Weigand SD, Shiung MM, Przybelski SA, O’Brien PC, Gunter JL, et al. Atrophy rates accelerate in amnestic mild cognitive impairment. Neurology 2008;70:1740–52. [PubMed: 18032747]
4. Fan Y, Resnick SM, Wu X, Davatzikos C, ADNI. Structural and functional biomarkers of prodromal Alzheimer’s disease: A high-dimensional pattern classification study. Neuroimage 2008;41:277–85. [PubMed: 18400519]
5. Minoshima S, Foster NL, Kuhl DE. Posterior cingulate cortex in Alzheimer’s disease. Lancet 1994;344:895. [PubMed: 7916431]

6. Herholz K, Salmon E, Perani D, Baron JC, Holthoff V, Frolich L, et al. Discrimination between Alzheimer dementia and controls by automated analysis of multicenter FDG PET. Neuroimage 2002;17:302–16. [PubMed: 12482085]
7. Mosconi L, Tsui WH, Herholz K, Pupi A, Drzezga A, Lucignani G, et al. Multicenter standardized ^{18}F-FDG PET diagnosis of mild cognitive impairment, Alzheimer's disease, and other dementias. J Nucl Med 2008;49:390–98. [PubMed: 18287270]
8. Minoshima S, Giordani B, Berent S, Frey KA, Foster NL, Kuhl DE. Metabolic reduction in the posterior cingulate cortex in very early Alzheimer's disease. Annal Neurol 1997;42:85–94. [PubMed: 9225689]
9. Nestor PJ, Fryer TD, Ikeda M, Hodges JR. Retrosplenial cortex (BA 29/30) hypometabolism in mild cognitive impairment (prodromal Alzheimer's disease). Eur J Neurosci 2003;18:2663–7. [PubMed: 14622168]
10. De Santi S, de Leon MJ, Rusinek H, Convit A, Tarshish CY, Roche A, et al. Hippocampal formation glucose metabolism and volume losses in MCI and AD. Neurobiol Aging 2001;22:529–39. [PubMed: 11445252]
11. de Leon MJ, Convit A, Wolf OT, Tarshish CY, DeSanti S, Rusinek H, et al. Prediction of cognitive decline in normal elderly subjects with 2-[(^{18})F]fluoro-2-deoxy-d-glucose/positron-emission tomography (FDG/PET). Proc Natl Acad Sci U S A 2001;98:10966–71. [PubMed: 11526211]
12. Drzezga A, Lautenschlager N, Siebner H, Riemenschneider M, Willoch F, Minoshima S, et al. Cerebral metabolic changes accompanying conversion of mild cognitive impairment into Alzheimer's disease: A PET follow-up study. Eur J Nucl Med Mol Imaging 2003;30:1104–13. [PubMed: 12764551]
13. Drzezga A, Grimmer T, Riemenschneider M, Lautenschlager N, Siebner H, Alexopoulus P, et al. Prediction of individual clinical outcome in MCI by means of genetic assessment and ^{18}F-FDG PET. J Nucl Med 2005;46:1625–32. [PubMed: 16204712]
14. Sowell ER, Peterson BS, Thompson PM, Welcome SE, Henkenius AL, Toga AW. Mapping cortical change across the human life span. Nat Neurosci 2003;6:309–15. [PubMed: 12548289]
15. Pardo JV, Sheikh SA, Scwindt G, Surerus-Johnsona C, Shaha H, Munch K, et al. Where the brain grows old: Decline in anterior cingulate and medial prefrontal function with normal aging. NeuroImage 2007;35:1231–37. [PubMed: 17321756]
16. Morris JC, Storandt M, Miller JP, McKeel DW, Price JL, Rubin EH, et al. Mild cognitive impairment represents early-stage Alzheimer disease. Arch Neurol 2001;58:397–405. [PubMed: 11255443]
17. Markesbery WR, Schmitt FA, Kryscio RJ, Davis DG, Smith CD, Wekstein DR. Neuropathologic substrate of mild cognitive impairment. Arch Neurol 2006;63:38–46. [PubMed: 16401735]
18. Anrnáiz E, Jelic V, Almkvist O, Wahlund L, Winblad B, Valind S, Nordberg A. Impaired cerebral glucose metabolism and cognitive functioning predict deterioration in mild cognitive impairment. Neuroreport 2001;12:851–5. [PubMed: 11277595]
19. Silverman DH, Small GW, Chang CY, Lu CS, Kung De Aburto MA, Chen W, et al. Positron emission tomography in evaluation of dementia: Regional brain metabolism and long-term outcome. JAMA 2001;286:2120–27. [PubMed: 11694153]
20. Ritchie K, Artero S, Touchon J. Classification criteria for mild cognitive impairment: A population-based validation study. Neurology 2001;56:37–42. [PubMed: 11148233]
21. Unverzagt FW, Sujuan G, Lane KA, Callahan C, Ogunniyi A, Baiyewu O, et al. Mild cognitive dysfunction: An epidemiological perspective with an emphasis on African Americans. J Geriatr Psychiatry Neurol 2007;20:215–26. [PubMed: 18004008]
22. Ganguli M, Dodge HH, Shen C, DeKosky ST. Mild cognitive impairment, amnestic type: An epidemiologic study. Neurology 2004;63:115–21. [PubMed: 15249620]
23. Li Y, Rinne JO, Mosconi L, Pirraglia E, Rusinek H, DeSanti S, et al. Regional analysis of FDG and PIB-PET images in normal aging, mild cognitive impairment, and Alzheimer's disease. Eur J Nucl Med Mol Imaging 2008;35:2169–81. [PubMed: 18566819]
24. Okello A, Edison P, Archer HA, Turkheimer FE, Kennedy J, Bullock R, et al. Microglial activation and amyloid deposition in mild cognitive impairment: A PET study. Neurology 2009;72:56–62. [PubMed: 19122031]

25. Mosconi L, Tsui WH, Pupi A, De Santi S, Drzezga A, Minoshima S, et al. ^{18}F-FDG PET database of longitudinally confirmed healthy elderly individuals improves detection of mild cognitive impairment and Alzheimer's disease. J Nucl Med 2007;48:1129–34. [PubMed: 17574982]
26. Knopman DS, Knudson D, Yoes ME, Weiss DJ. Development and standardization of a new telephonic cognitive screening test: The Minnesota Cognitive Acuity Screen (MCAS). Neuropsychiatry Neuropsychol Behav Neurol 2000;13:286–96. [PubMed: 11186165]
27. Minoshima S, Berger KL, Lee KS, Mintun MA. An automated method for rotational correction and centering of three-dimensional functional brain images. J Nucl Med 1992;33:1579–85. [PubMed: 1634959]
28. Minoshima S, Koeppe RA, Frey KA, Kuhl DE. Anatomic standardization: Linear scaling and nonlinear warping of functional brain images. J Nucl Med 1994;35:1528–37. [PubMed: 8071705]
29. Minoshima S, Frey KA, Koeppe RA, Foster NL, Kuhl DE. A diagnostic approach in Alzheimer's disease using three-dimensional stereotactic surface projections of ^{18}F-FDG PET. J Nucl Med 1995;36:1238–48. [PubMed: 7790950]
30. Lee JT, Munch KR, Carlis JV, Pardo JV. Internet image viewer (iiV). BMC Med Imaging 2008;8:10. [PubMed: 18510765]
31. Joachims, T. Making large-scale SVM learning practical. In: Scholkopf, B.; Burges, C.; Smola, A., editors. Advances in kernel methods: Support vector learning. Boston: MIT Press; 1999. p. 185-208.
32. Chang, CC.; Lin, CJ. LIBSVM: A library for support vector machines. [Accessed May 7, 2009]. Last updated February 27, 2009; http://140.112.30.28/~cjlin/papers/libsvm.pdf
33. Guyon, I.; Gunn, S.; Nikravesh, M.; Zadeh, LA., editors. Studies in fuzziness and soft computing. Vol. 207. Berlin: Springer-Verlag; 2006. Feature extraction foundations and applications.
34. Lancaster JL, Woldorff MG, Parsons LM, Liotti M, Freitas CS, Rainey L, et al. Automated Talairach atlas labels for functional brain mapping. Hum Brain Mapp 2000;10:120–31. [PubMed: 10912591]
35. Kurani, AS.; Xu, DH.; Furst, J.; Raicu, DS. Co-occurrence matrices for volumetric data. In: Hamza, MH., editor. Proceedings computer graphics and imaging. Anaheim: Acta Press; 2004. p. 447-52.
36. Barker WW, Luis CA, Kashuba A, Luis M, Harwood DG, Loewenstein D, et al. Relative frequencies of Alzheimer disease, Lewy body, vascular and frontotemporal dementia, and hippocampal sclerosis in the state of Florida brain bank. Alzheimer Dis Assoc Disord 2002;16:203–12. [PubMed: 12468894]
37. Hunderfund AL, Roberts RO, Slusser TC, Leibson CL, Geda YE, Ivnik RJ, et al. Mortality in amnestic mild cognitive impairment: A prospective community study. Neurology 2006;67:1764–8. [PubMed: 17130407]

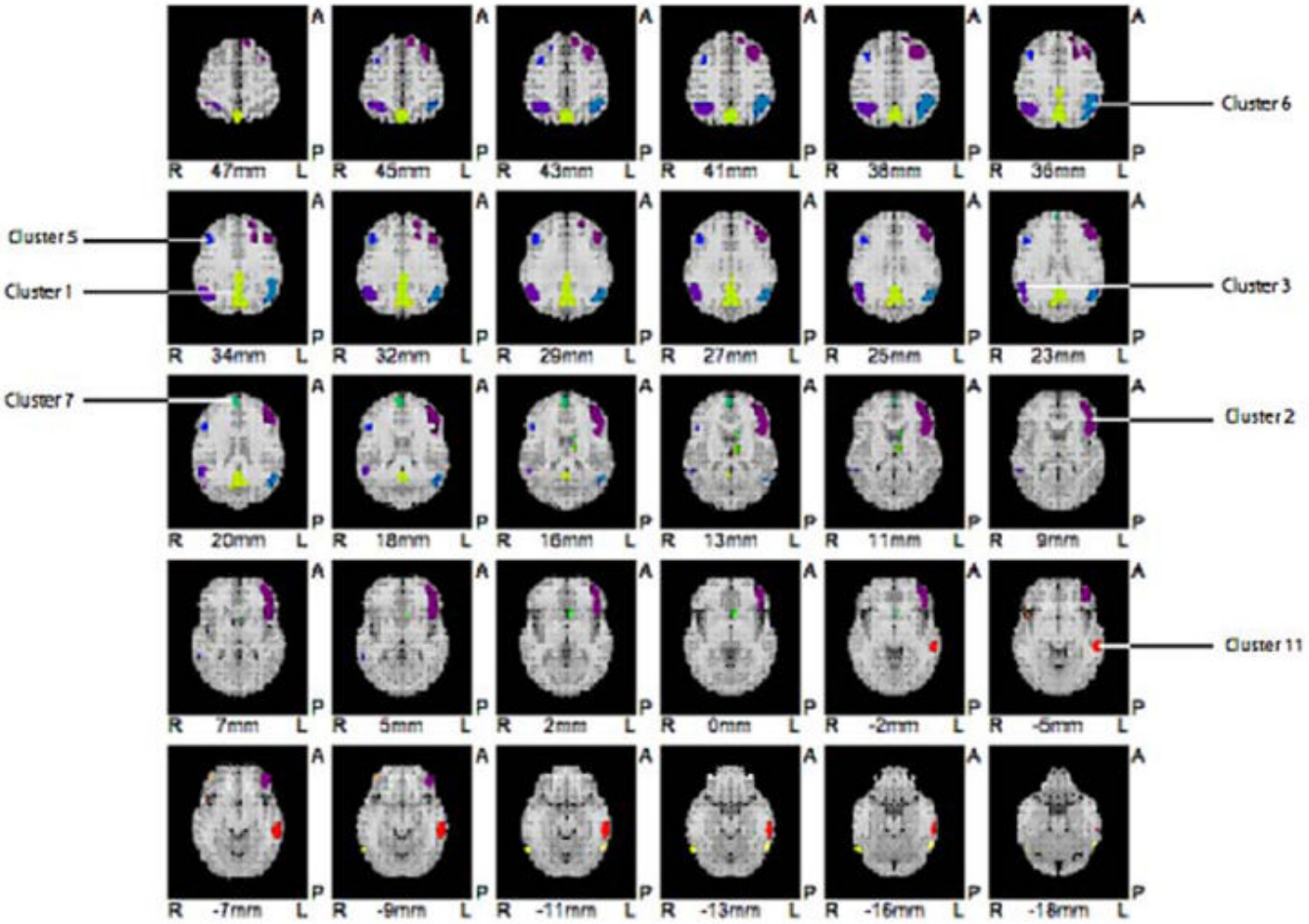

Figure 1.
Cluster division for SVM based on the subtraction of FDG PET scans of healthy controls from all MCI patients after age regression (i.e., MCI template). Note the similarity to AD pattern. Top of image is anterior; image left is patient's right side. Each cluster has been colorized to aid in identification.

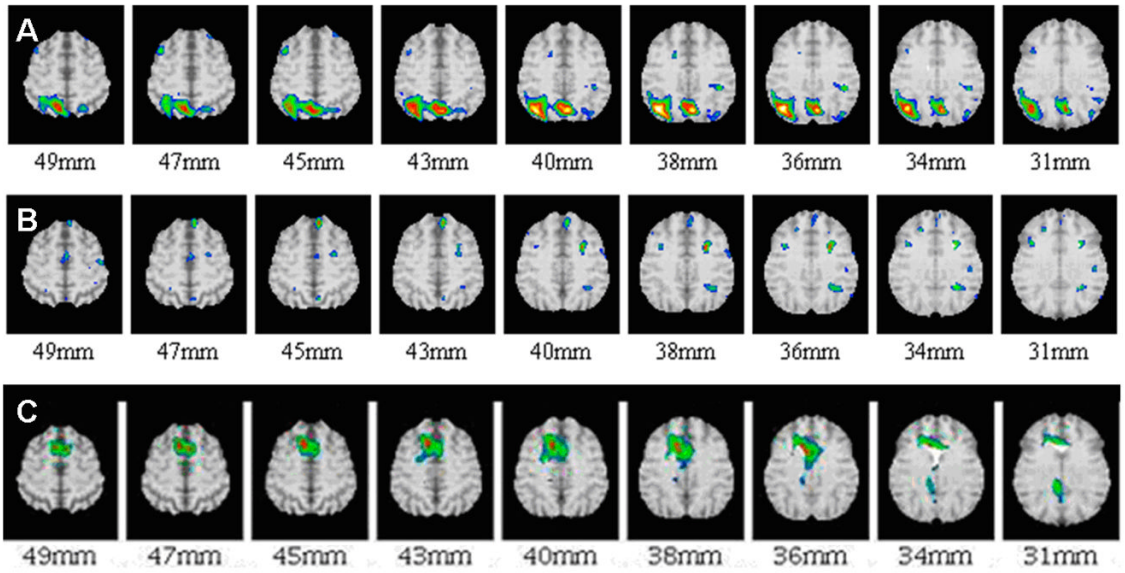

Figure 2.
Examples of FDG PET difference images between different individual MCI patients vs. controls showing examples of presence (A) and absence (B) of an AD-like pattern as well as one with an FTD pattern (C). The numbers indicate millimeters above the AC-PC plane. Orientation same as in Figure 1.

Table 1

Initial PET findings and diagnoses of MCI patients at three years of follow-up.

Scan #	Initial Diagnosis	Reading (JVP)	Reading (MAK)	Diagnosis on follow-up
p0024	MCI, Amnestic	AD	FTD	Probable AD†‡
p0025	MCI, Amnestic	HC	AD	MCI, Amnestic†
p0043	MCI, Amnestic	AD	HC	Probable AD
p0046	MCI, Amnestic	HC	FTD	Probable AD
p0047	MCI, Amnestic	AD	AD	MCI, Amnestic
p0078	MCI, non-Amnestic, multidomain	AD	AD	Definite LBD†‡
p0083	MCI, non-Amnestic	AD	HC	Dementia, NOS†‡
p0093	MCI, NOS	AD	AD	Probable LBD†
p0094	MCI, Amnestic, multidomain	HC	HC	Probable AD
p0099	MCI, Amnestic, 1 domain	HC	AD	Probable AD
p0100	MCI, NOS	FTD	AD/FTD	Probable FTD‡
p0102	MCI, Amnestic	HC	HC	Possible AD
p0103	MCI, non-Amnestic	HC	AD	MCI, non-amnestic, Stable
p0106	MCI, Amnestic, multidomain	HC	HC	Possible AD
p0111	MCI, non-Amnestic, multidomain	HC	AD	Probable FTD
p0112	MCI, non-Amnestic, 1 domain	HC	AD	MCI, Non-amnestic, 1 domain
p0113	MCI, Amnestic, multidomain	Artifact	AD	Probable AD
p0115	MCI, Amnestic, multidomain	HC	AD	Probable AD
p0116	MCI, nonAmnestic, multidomain	HC	FTD	MCI, Non-amnestic, multidomain

† AD-like pattern used for SVM analysis;

‡ deceased; NOS, not otherwise specified; HC, healthy control.

Table 2

Concordance of classification by two blinded raters of FDG PET difference images (MCI patient minus controls).

Interpreter	Initial diagnostic classification	Sample Size, N	Normal PET	AD PET	FTD PET
JVP*	MCI	19	11	6	1
MAK	MCI	19	5	10	4
JVP	Normal	27	22	2	3
MAK	Normal	27	22	3	2

* one subject's scan rated as artifactual.